

Spectral and Raman Analysis of Eu^{3+} Doped in Zinc Lithium Cadmium Magnesium Borophosphate Glasses

S.L.Meena

Ceramic Laboratory, Department of physics, Jai Narain Vyas University, Jodhpur 342001(Raj.) India

Abstract

Glass sample of Zinc Lithium Cadmium Magnesium Borophosphate $(40-x)\text{P}_2\text{O}_5:10\text{ZnO}:10\text{Li}_2\text{O}:10\text{CdO}:10\text{MgO}:20\text{B}_2\text{O}_3:x\text{Eu}_2\text{O}_3$ (where $x=1,1.5,2$ mol%) have been prepared by melt-quenching technique. The amorphous nature of the prepared glass samples was confirmed by X-ray diffraction. The absorption, fluorescence and raman spectra of three Eu^{3+} doped zinc lithium cadmium magnesium borophosphate glasses have been recorded at room temperature. The various interaction parameters like Slater-Condon parameters F_k ($k=2,4,6$), Lande parameter (ξ_{4f}), nephelauxetic ratio (β'), bonding parameter ($b^{1/2}$) and Racah parameters E^k ($k=1,2,3$) have been computed. Judd-Ofelt intensity parameters and laser parameters have also been calculated.

Keywords: ZLCMBP glasses, Energy interaction parameters, Optical properties, Raman analysis.

Date of Submission: 06-02-2022

Date of Acceptance: 19-02-2022

I. Introduction

Glasses with dopants of rare earth ions have continuously drawn the attention through their potential applications in solid state lasers, optical Amplifiers and sensor fields [1-5].

Recently, phosphate glasses have received a great deal of attention due to their potential applications in laser technologies and optical data transmission, sensors and energy solar cell [6-10]. Phosphate glasses doped with a transition metal or rare-earth ions are considered as valuable materials for both optical and electrical applications [11,12]. The addition of CdO improves the physical and chemical properties of the glass [13,14]. ZnO is a wide band gap semiconductor and has received increasing research interest. It is an important multifunctional material due to its specific chemical, surface and microstructural properties [15, 16]. Phosphate glasses have a low glass transition temperature, high coefficient of thermal expansion, low melting temperature and high gain density. The high gain density in phosphate glasses is due to high solubility of rare earth ions in phosphate network. These characteristics are known to have some influences on various factors such as the preparation temperature, nature and the composite type. The relatively poor chemical durability of some specific types of phosphate glasses has played the role in limiting their practical applications. This disadvantage can be solved by the addition of some transition metal ions or alkaline earth as well as intermediate oxides to the host glass [17-19].

The aim of the present study is to prepare the Eu^{3+} doped zinc lithium cadmium magnesium borophosphate glass with different Eu_2O_3 concentrations. The absorption, fluorescence and raman spectra of Eu^{3+} of the glasses were investigated. The Judd-Ofelt theory has been applied to compute the intensity parameters Ω_λ ($\lambda=2, 4, 6$). These intensity parameter have been used to evaluate optical properties such as spontaneous emission probability, branching ratio, radiative life time and stimulated emission cross section.

II. Experimental Techniques

Preparation of glasses

The following Eu^{3+} doped borophosphate glass samples $(40-x)\text{P}_2\text{O}_5:10\text{ZnO}:10\text{Li}_2\text{O}:10\text{CdO}:10\text{MgO}:20\text{B}_2\text{O}_3:x\text{Eu}_2\text{O}_3$ (where $x=1,1.5, 2$) have been prepared by melt-quenching method. Analytical reagent grade chemical used in the present study consist of P_2O_5 , ZnO, Li_2O , CdO, MgO, B_2O_3 and Eu_2O_3 . They were thoroughly mixed by using an agate pestle mortar. then melted at 1065°C by an electrical muffle furnace for 2h., After complete melting, the melts were quickly poured in to a preheated stainless steel mould and annealed at temperature of 350°C for 2h to remove thermal strains and stresses. Every time fine powder of cerium oxide was used for polishing the samples. The glass samples so prepared were of good optical quality and were transparent. The chemical compositions of the glasses with the name of samples are summarized in Table 1.

Table 1

Chemical composition of the glasses

Sample	Glass composition (mol %)
ZLCMBP(UD)	40P ₂ O ₅ :10ZnO:10Li ₂ O:10CdO:10MgO:20B ₂ O ₃
ZLCMBP(EU1)	39P ₂ O ₅ :10ZnO:10Li ₂ O:10CdO:10MgO:20B ₂ O ₃ :1Eu ₂ O ₃
ZLCMBP(EU1.5)	38.5P ₂ O ₅ :10ZnO:10Li ₂ O:10CdO:10MgO:20B ₂ O ₃ :1.5Eu ₂ O ₃
ZLCMBP(EU2)	38P ₂ O ₅ :10ZnO:10Li ₂ O:10CdO:10MgO:20B ₂ O ₃ :2Eu ₂ O ₃

ZLCMBP(UD) -Represents undoped Zinc Lithium Cadmium Magnesium Borophosphate glass specimen.

ZLCMBP(EU) -Represents Eu^{3+} doped Zinc Lithium Cadmium Magnesium Borophosphate glass specimens.

III. Theory

3.1 Oscillator Strength

The spectral intensity is expressed in terms of oscillator strengths using the relation [20].

$$f_{\text{expt.}} = 4.318 \times 10^{-9} \int \varepsilon(\nu) d\nu \quad (1)$$

Where, $\varepsilon(\nu)$ is molar absorption coefficient at a given energy ν (cm^{-1}), to be evaluated from Beer–Lambert law. Under Gaussian Approximation, using Beer–Lambert law, the observed oscillator strengths of the absorption bands have been experimentally calculated [21], using the modified relation:

$$P_m = 4.6 \times 10^{-9} \times \frac{1}{cl} \log \frac{I_0}{I} \times \Delta\nu_{1/2} \quad (2)$$

Where c is the molar concentration of the absorbing ion per unit volume, l is the optical path length, $\log I_0/I$ is optical density and $\Delta\nu_{1/2}$ is half band width.

3.2. Judd-Ofelt Intensity Parameters

According to Judd [22] and Ofelt [23] theory, independently derived expression for the oscillator strength of the induced forced electric dipole transitions between an initial J manifold $|4f^N(S, L) J\rangle$ level and the terminal J' manifold $|4f^N(S', L') J'\rangle$ is given by:

$$\frac{8\pi^2 mc \nu}{3h(2J+1)n} \left[\frac{(n^2+2)^2}{9} \right] \times S(J, J') \quad (3)$$

Where, the line strength $S(J, J')$ is given by the equation

$$S(J, J') = e^2 \sum_{\lambda=2,4,6} \Omega_{\lambda} \langle 4f^N(S, L) J \| U^{(\lambda)} \| 4f^N(S', L') J' \rangle^2$$

In the above equation m is the mass of an electron, c is the velocity of light, ν is the wave number of the transition, h is Planck's constant, n is the refractive index, J and J' are the total angular momentum of the initial and final level respectively, Ω_{λ} ($\lambda = 2, 4, 6$) are known as Judd-Ofelt intensity parameters.

3.3 Radiative Properties

The Ω_{λ} parameters obtained using the absorption spectral results have been used to predict radiative properties such as spontaneous emission probability (A) and radiative life time (τ_R), and laser parameters like fluorescence branching ratio (β_R) and stimulated emission cross section (σ_p).

The spontaneous emission probability from initial manifold $|4f^N(S', L') J'\rangle$ to a final manifold $|4f^N(S, L) J\rangle$ is given by:

$$A[(S', L') J'; (S, L) J] = \frac{64\pi^2 \nu^3}{3h(2J'+1)} \left[\frac{n(n^2+2)^2}{9} \right] \times S(J', J) \quad (4)$$

Where, $S(J', J) = e^2 [\Omega_2 \| U^{(2)} \|^2 + \Omega_4 \| U^{(4)} \|^2 + \Omega_6 \| U^{(6)} \|^2]$

The fluorescence branching ratio for the transitions originating from a specific initial manifold $|4f^N(S', L') J' \rangle$ to a final many fold $|4f^N(S, L) J \rangle$ is given by

$$\beta[(S', L') J'; (S, L) J] = \sum_{S L J} \frac{A[(S' L)]}{A[(S' L') J' (\bar{S} \bar{L})]} \quad (5)$$

Where, the sum is over all terminal manifolds.

The radiative life time is given by

$$\tau_{rad} = \sum_{S L J} A[(S', L') J'; (S, L) J] = A_{Total}^{-1} \quad (6)$$

Where, the sum is over all possible terminal manifolds. The stimulated emission cross-section for a transition from an initial manifold $|4f^N(S', L') J' \rangle$ to a final manifold $|4f^N(S, L) J \rangle$ is expressed as

$$\sigma_p(\lambda_p) = \left[\frac{\lambda_p^4}{8\pi c n^2 \Delta\lambda_{eff}} \right] \times A[(S', L') J'; (\bar{S}, \bar{L}) \bar{J}] \quad (7)$$

Where, λ_p the peak fluorescence wavelength of the emission band and $\Delta\lambda_{eff}$ is the effective fluorescence line width.

3.4 Nephelauxetic Ratio (β) and Bonding Parameter ($b^{1/2}$)

The nature of the R-O bond is known by the Nephelauxetic Ratio (β') and Bonding Parameter ($b^{1/2}$), which are computed by using following formulae [24, 25]. The Nephelauxetic Ratio is given by

$$\beta' = \frac{\nu_g}{\nu_a} \quad (8)$$

where, ν_g and ν_a refer to the energies of the corresponding transition in the glass and free ion, respectively. The values of bonding parameter ($b^{1/2}$) is given by

$$b^{1/2} = \left[\frac{1-\beta'}{2} \right]^{1/2} \quad (9)$$

IV. Result and Discussion

4.1 XRD Measurement

Figure 1 presents the XRD pattern of the sample contain - P₂O₅ which is show no sharp Bragg's peak, but only a broad diffuse hump around low angle region. This is the clear indication of amorphous nature within the resolution limit of XRD instrument.

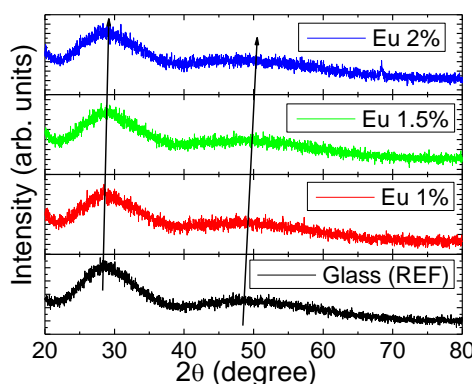


Fig.1: X-ray diffraction pattern of ZLCMBP (EU) glasses.

4.2 Raman spectra

The Raman spectrum of Zinc Lithium Cadmium Magnesium Borophosphate (ZLCMBP) glass specimens is recorded and is shown in Fig. 2. The spectrum peaks located at 397 and 779 cm⁻¹. The band at 397 cm⁻¹ is related to the bending motion of phosphate polyhedral PO₄ units with cation like ZnO as the modifier. The broad band at 779 cm⁻¹ is due to symmetric stretching of (P-O-P) bridging oxygen bonds in (P₂O₇)₄ units.

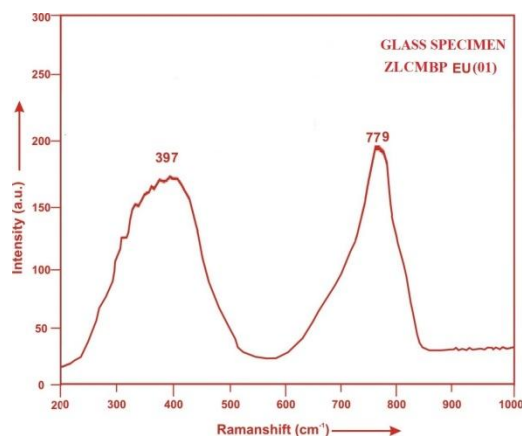


Fig.2: Raman spectrum of ZLCMBP EU (01) glass.

4.3 Absorption Spectrum

The absorption spectra of Eu^{3+} doped ZLCMBP(EU 01) glass specimen has been presented in Figure 3 in terms of optical density versus wavelength (nm). Four absorption bands have been observed from the ground state ${}^7\text{F}_0$ to excited states ${}^5\text{D}_2$, ${}^5\text{L}_6$, (${}^5\text{G}_2$, ${}^5\text{G}_4$, ${}^5\text{G}_6$) and ${}^5\text{D}_4$ for Eu^{3+} doped ZLCMBP glasses.

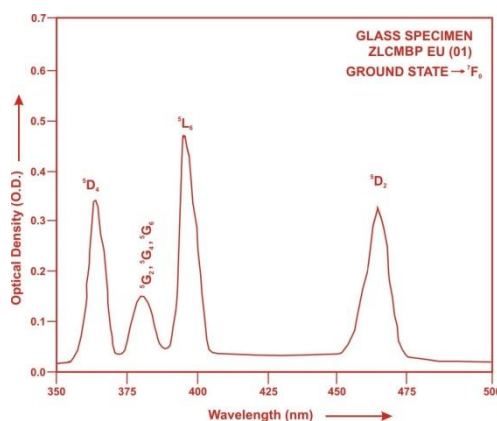


Fig.3: Absorption spectrum of ZLCMBP EU(01)glass.

The experimental and calculated oscillator strengths for Eu^{3+} ions in zinc lithium cadmiummagnesium borophosphate glasses are given in Table 2.

Table2: Measured and calculated oscillator strength ($P_m \times 10^{+6}$) of Eu^{3+} ions in ZLCMBP glasses.

Energy level ${}^7\text{F}_0$	Glass ZLCMBP(EU01)		Glass ZLCMBP(EU1.5)		Glass ZLCMBP(EU02)	
	P_{exp}	P_{cal}	P_{exp}	P_{cal}	P_{exp}	P_{cal}
${}^3\text{D}_2$	2.26	2.36	2.23	2.35	2.20	2.32
${}^3\text{L}_6$	3.68	3.80	3.66	3.79	3.62	3.77
${}^5\text{G}_2, {}^5\text{G}_4, {}^5\text{G}_6$	0.83	0.95	0.81	0.95	0.79	0.94
${}^3\text{D}_4$	3.02	3.15	2.99	3.14	2.96	3.12
r.m.s. deviation	0.1156		0.1344		0.1469	

The small value of r.m.s. deviation indicates fairness of fitting between experimental and calculated oscillator strengths.

Computed values of F_2 , Lande' parameter (ξ_{4f}), Nephlauxetic ratio (β') and bonding parameter ($b^{1/2}$) for Eu^{3+} doped ZLCMBP glass specimen are given in Table 3.

Table 3. F_2, ξ_{4f}, β' and $b^{1/2}$ parameters for Europium doped glass specimen.

Glass Specimen	F_2	ξ_{4f}	β'	$b^{1/2}$
Eu^{3+}	372.63	1445.73	0.9645	0.1332

In the present case the three Ω_2 parameters follow the trend $\Omega_2 > \Omega_4 > \Omega_6$. The spectroscopic quality factor (Ω_4/Ω_6) related with the rigidity of the glass system has been found to lie between 1.069 and 1.072 in the present glasses.

The value of Judd-Ofelt intensity parameters are given in **Table 4**

Table 4:Judd-Ofelt intensity parameters for Eu^{3+} doped ZLCMBP glass specimens.

Glass Specimen	$\Omega_2(\text{pm}^2)$	$\Omega_4(\text{pm}^2)$	$\Omega_6(\text{pm}^2)$	Ω_4/Ω_6	Trend	References
ZLCMBP(EU01)	4.649	3.509	3.274	1.072	$\Omega_2 > \Omega_4 > \Omega_6$	P.W.
ZLCMBP(EU1.5)	4.618	3.496	3.271	1.069	$\Omega_2 > \Omega_4 > \Omega_6$	P.W.
ZLCMBP(EU02)	4.576	3.474	3.244	1.071	$\Omega_2 > \Omega_4 > \Omega_6$	P.W.
LSBP(DY)	5.24	2.32	1.97	1.178	$\Omega_2 > \Omega_4 > \Omega_6$	[18]
PKAICAF(EU)	7.49	6.30	0.50	12.60	$\Omega_2 > \Omega_4 > \Omega_6$	[22]
NSGP(DY)	12.38	6.31	3.20	1.972	$\Omega_2 > \Omega_4 > \Omega_6$	[23]
NSGP(EU)	15.65	10.00	8.12	1.232	$\Omega_2 > \Omega_4 > \Omega_6$	[23]

From Table 4 it is observed that Ω_2 parameter is high. The Ω_2 parameter depends generally on the asymmetry of the sites in the neighborhood of rare earth ion. The higher the Ω_2 parameter the higher is the degree of asymmetry around the rare earth ion and stronger the covalency of rare earth ion-oxygen bond.

4.4. Fluorescence Spectrum

The fluorescence spectrum of Eu^{3+} doped in zinc lithium cadmiummagnesium borophosphate glass is shown in Figure 4. There are three broad bands observed in the Fluorescence spectrum of Eu^{3+} doped zinc lithium cadmiummagnesium borophosphate glass. The wavelengths of these bands along with their assignments are given in Table 5. Fig. (4). Shows the fluorescence spectrum with seven peaks (${}^5\text{D}_0 \rightarrow {}^7\text{F}_0$), (${}^5\text{D}_0 \rightarrow {}^7\text{F}_1$), (${}^5\text{D}_0 \rightarrow {}^7\text{F}_2$), (${}^5\text{D}_0 \rightarrow {}^7\text{F}_3$), (${}^5\text{D}_0 \rightarrow {}^7\text{F}_4$), (${}^5\text{D}_0 \rightarrow {}^7\text{F}_5$) and (${}^5\text{D}_0 \rightarrow {}^7\text{F}_6$) for glass specimens.

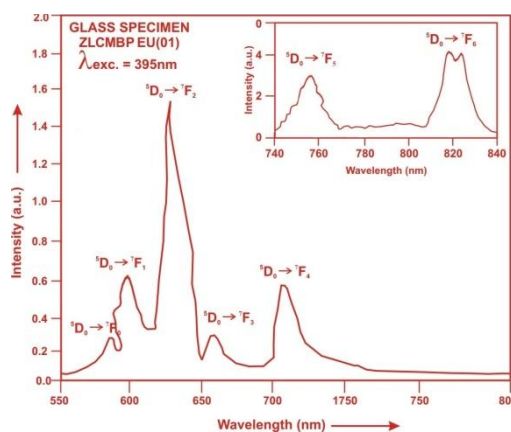


Fig.4: fluorescence spectrum of ZLCMBP EU (01) glass.

Table 5. Emission peak wave lengths (λ_{max}), radiative transition probability (A_{rad}), branching ratio (β), stimulated emission cross-section (σ_p) and radiative life time (τ_R) for various transitions in Eu^{3+} doped ZLCMBP glasses.

Transition	ZLCMBPEU 01					ZLCMBPEU 1.5				ZLCMBPEU 02			
	λ_{max} (nm)	$A_{\text{rad}}(\text{s}^{-1})$	β	$\sigma_p (10^{-20} \text{cm}^2)$	$\tau_R(\mu\text{s})$	$A_{\text{rad}}(\text{s}^{-1})$	β	$\sigma (10^{-20} \text{cm}^2)$	$\tau_R(\mu\text{s})$	$A_{\text{rad}}(\text{s}^{-1})$	β	$\sigma_p (10^{-20} \text{cm}^2)$	$\tau_R(\mu\text{s})$
${}^5\text{D}_0 \rightarrow {}^7\text{F}_2$	615	46.626	0.2676	0.0153	5738.79	46.428	0.2671	0.0150	5752.69	46.073	0.2664	0.0147	5782.97
${}^5\text{D}_0 \rightarrow {}^7\text{F}_4$	710	127.13	0.7296	0.0675		126.90	0.7300	0.0670		126.35	0.7307	0.0657	
${}^5\text{D}_0 \rightarrow {}^7\text{F}_6$	820	0.4997	0.0029	0.000317		0.5001	0.0029	0.000314		0.4971	0.0029	0.000310	

V. Conclusion

In the present study, the glass samples of composition $(40-x) \text{P}_2\text{O}_5:10\text{ZnO}:10\text{Li}_2\text{O}:10\text{CdO}:10\text{MgO}:20\text{B}_2\text{O}_3: x \text{Eu}_2\text{O}_3$ (where $x=1, 1.5, 2\text{mol} \%$) have been prepared by melt-quenching method. The Judd-Ofelt theory has been applied to calculate the oscillator strength and intensity parameters $\Omega_\lambda (\lambda=2, 4, 6)$. The radiative transition rate and the branching ratio are highest for (${}^5\text{D}_0 \rightarrow {}^7\text{F}_4$) transition and hence it is useful for laser action. The stimulated emission cross section (σ_p) value is also very high for the transition (${}^5\text{D}_0 \rightarrow {}^7\text{F}_4$). This shows that (${}^5\text{D}_0 \rightarrow {}^7\text{F}_4$) transition is most probable transition.

References

- [1]. Kothandan, D. and Kumar, R.J. (2015). Optical properties of rare earth doped borate glasses, Int. J. Chem. Tech. Research 8(6), 310-314.
- [2]. Pawar, P. P., Munishwar, S.R. and Gedam, R.S. (2016). Physical and optical properties of $\text{Dy}^{3+}/\text{Pr}^{3+}$ co-doped lithium borate glasses for W-LED, J. Alloys and Compounds, 660, 347-355.

- [3]. Monisha, M., Nancy, A., Souza, D., Jegde, V., Prabhu, N.S. and Sayyed, M.I. (2020). Dy³⁺ doped SiO₂- B₂O₃-Al₂O₃-NaF-ZnF₂ glasses, An exploration of optical and gamma radiation shielding features, *Current Applied Physics* 20(11), 1207-1210.
- [4]. Damodaraiah, S., Prasad, V. R., Lakshmi, R.P.V. and Ratnakaram, Y.C. (2019). Luminescence behaviour and phonon sideband analysis of europium doped Bi₂O₃ based phosphate glasses for red emitting device applications, *Opt. Mat.* 92, 352-358.
- [5]. Kaur, R., Khanna, A. (2020). Photoluminescence and thermal properties of trivalent ion-doped lanthanum tellurite anti-glass composite samples, *J. Lum.*, 117375.
- [6]. Deepa, A.V., Kumar, P. V., Moorthy, K. S., Murlimanohar, P., Mohapatra, M., Kumar S. P. and Murugasen, P. (2020). Optical, electrical, mechanical properties of Pr³⁺ and Yb³⁺ doped phosphate glass, *Opt. and Quant. Electronics* 52.
- [7]. Deepa, A. V., Murugasen, P., Muralimanohar, P., Sathyamoorthy, K., Kumar, P. V. (2019). A comparison on the structural and optical properties of different rare earth doped phosphate glass, *Optik*, 181, 361-367.
- [8]. Mandal, P., Chowdhary, S. and Ghosh, S. (2019). Spectroscopic characterization of Er³⁺ doped lead zinc phosphate glass via Judd-Ofelt analysis, *Bullet. Mat. Science* 42.
- [9]. Chowdhury, S., Mandal, P., Ghosh, S. (2019). Structural properties of Er³⁺ doped lead zinc phosphate glasses, *Mat. Sci. and Eng.*, 240, 116-120.
- [10]. El Maaref, A.A., Badr, S., Shaaban, Kh.S., Wahab, E.A. A. and Elokr, M.M. (2019). Optical properties and radiative rates of Nd³⁺ doped zinc-sodium phosphate glasses, *Journal of rare Earth*, 37, 253-259.
- [11]. Karabulut, M., Metwalli, E., Day, D.E. and Brow, R.K. (2003). Mossbauer and IR investigation of iron ultraphosphate glasses, *J. Non-Cryst. Solids*, 328(1-3), 199-206.
- [12]. Ehrhart, D. (2015). Phosphate and fluoride phosphate optical glasses Properties, structure and applications, *Physics and Chemistry of Glasses: European J. Glass Science and Tech. Part B*, 56(6), 217-234.
- [13]. Ghos, Alok, Ghos, A. (2007). Optical and other physical properties of semiconducting cadmium vanadate glasses, *J. App. Phy.* 101, 083511.
- [14]. Balakrishna, A., Rajesh, D. and Ratnakaram, Y.C. (2013). Structural and optical properties of Nd³⁺ in lithium fluoro-borate glass with relevant modifier oxides. *Opt. Mater.*, 35, 2670-2676.
- [15]. Bobkova, N.M. and Khot, S.A. (2005). Zinc oxide in borate glass-forming systems. *J. Glass and ceramics*, 62, 170.
- [16]. Pal, M., Roy, B. and Pal, M. (2011). Structural characterization of borate glasses containing zinc and manganese oxide. *J. Mod. Physics*, 2, 1062-66.
- [17]. Jimenez, J. A. (2014). Emission properties of Sm²⁺ and Sm³⁺ co doped Barium phosphate Glass, *J. Elect. materials* 43(9), 3588-3592.
- [18]. Chandrasekhar, A. V., Radhahathy, A., Reddy, B.J., Reddy, Y.P., Ramamoorthy, L., Ravikumar, RVSSN (2003). Optical Absorption spectrum of dysprosium doped zinc phosphate glass, *Optical materials* 22(3), 215-220.
- [19]. Pisarska, J., Sottys, M., Zur, L., Pisarski, W. A., Jaya sankar, C.K. (2014). Excitation and luminescence of earth doped lead phosphate glasses, *App. physics B* 116(4), 837-845.
- [20]. Gorller-Walrand, C. and Binnemans, K. (1988). Spectral Intensities of f-f Transition. In: Gshneider Jr., K.A. and Eyring, L., Eds., *Handbook on the Physics and Chemistry of Rare Earths*, Vol. 25, Chap. 167, North-Holland, Amsterdam, 101.
- [21]. Sharma, Y.K., Surana, S.S.L. and Singh, R.K. (2009). Spectroscopic Investigations and Luminescence Spectra of Sm³⁺ Doped Soda Lime Silicate Glasses. *Journal of Rare Earths*, 27, 773.
- [22]. Judd, B.R. (1962). Optical Absorption Intensities of Rare Earth Ions. *Physical Review*, 127, 750.
- [23]. Ofelt, G.S. (1962). Intensities of Crystal Spectra of Rare Earth Ions. *The Journal of Chemical Physics*, 37, 511.
- [24]. Sinha, S.P. (1983). Systematics and properties of lanthanides, Reidel, Dordrecht.
- [25]. Krupke, W.F. (1974). *IEEE J. Quantum Electron* QE, 10, 450.
- [26]. Vijayakumar, R., Venkataiah, G. and Marimuthu, K. (2015). Structural and luminescence studies on Dy³⁺ doped boro-phosphate glasses for white LED's and laser applications. *J. Alloy Compd.* 625, 234-243.
- [27]. Rasool, S.N., Moorthy, L.R. and Jayasankar, C.K. (2013). Optical and luminescence properties of Eu³⁺ -doped. *Mater. Express* 3(3), 1-10.
- [28]. Shoaib, M., Chanthima, N., Rooh, G., Rajaramkrishna, R. and Kaewkhao, J. (2019). Physical and luminescence properties of rare earth doped phosphate glasses for solid state lighting applications, *14(3)*, 20-26.

S.L.Meena. "Spectral and Raman Analysis of Eu³⁺ Doped in Zinc Lithium Cadmium Magnesium Borophosphate Glasses." *IOSR Journal of Applied Physics (IOSR-JAP)*, 14(01), 2022, pp. 39-44.